From trees to rain: Enhancement of cloud glaciation and precipitation by pollen

Authors: Jan Kretzschmar[1*], Mira Pöhlker[2,1], Frank Stratmann[2], Heike Wex[2], Christian Wirth[3,4,] Johannes Quaas[1,3]

Affiliations:

[1]Institute for Meteorology, Leipzig University; 04103 Leipzig, Germany

[2]Leibniz-Institute for Tropospheric Research; 04318 Leipzig, Germany

[3]German Centre for Integrative Biodiversity Research (iDiv) Halle-Jena-Leipzig; 04103 Leipzig, Germany

[4]Max-Planck-Institute for Biogeochemistry; 07745 Jena, Germany

*Corresponding author. Email: jan.kretzschmar@uni-leipzig.de

Abstract: The ability of pollen to enable the glaciation of supercooled liquid water has been demonstrated in laboratory studies; however, the potential large-scale effect of trees and pollen on clouds, precipitation and climate is pressing knowledge to better understand and project clouds in the current and future climate. Combining ground-based measurements of pollen concentrations and satellite observations of cloud properties within the United States, we show that enhanced pollen concentrations during springtime lead to a higher cloud ice fraction. We further establish the link from the pollen-induced increase in cloud ice to a higher precipitation frequency. In light of anthropogenic climate change, the extended and strengthened pollen season and future alterations in biodiversity can introduce a localized climate forcing and a modification of the precipitation frequency and intensity.

One-Sentence Summary: Enhanced amount of cloud ice and precipitation in presence of airborne pollen.

Clouds may consist of supercooled liquid water in a temperature range between 0 °C and –38 °C. Whether or not the cloud glaciates in this temperature regime depends on the availability of a subset of atmospheric aerosol particles, the ice nucleating particles (INP), which enable the freezing of supercooled liquid droplets or haze particles via heterogeneous freezing mechanisms. The thermodynamic state of clouds is of particular importance for their propensity to form rain. The vast majority of rain events originate from ice clouds *(1,2)*. It has been demonstrated that pollen are among the aerosol species that may serve as INP *(3-8)*. While the contribution of pollen to the glaciation of mixed-phase clouds is thought to be rather small on a global scale compared to other INP like dust, they can nevertheless play an important role on regional and seasonal scales *(6,9)*.

Laboratory studies, investigating the freezing temperature of supercooled water droplets with an embedded pollen grain indicate that most pollen may induce freezing in a temperature range between -15 °C and -25 °C *(10)*. To reach this temperature regime, pollen have to be transported into higher layers of the atmosphere where such temperatures are reached. Ground-based lidar observations have revealed that layers containing pollen may reach those temperature regimes, being lifted by vertical mixing due to convection and turbulence, or due to large-scale uplift *(11)*. Due to their relatively large size, whole pollen grains have a limited residence time in the atmosphere before they are removed by gravitational settling *(12,13)*.

However, it is not the whole pollen grain itself but rather macromolecules on their surface that act as INP *(e.g., 6,7,14-16)*. Under humid conditions, pollen grains rupture into sub-pollen particles. Due to their smaller size, these particles have a longer residence time in the atmosphere and can reach higher altitudes than a whole pollen grain, increasing their ability to act as INP in the mixed-phase temperature regime *(6,13,17)*.

While the ice activity of pollen is widely researched in laboratory studies, so far there is no evidence on the role of pollen for cloud glaciation from observations at a large scale. In this study, we, therefore, aim at assessing whether the effect of pollen on the cloud ice fraction in the heterogeneous freezing temperature regime can be quantified using ground-based pollen concentration and satellite observations of clouds and whether this induces an increased precipitation frequency in mixed-phase clouds as illustrated in Fig. 1.

Results:

As a proxy for pollen concentration in the atmosphere, we employ ground-based pollen concentration observations, collected from stations within the United States (US; the location of pollen stations used is given in fig. S1). Data from these pollen stations are disseminated by the National Allergy Bureau (NAB), which is part of the American Academy of Allergy, Asthma and Immunology (AAAAI). In this study, we use pollen concentrations collected by more than 50 surface stations from 2007 to 2016. These stations use volumetric air samplers from which the daily pollen concentrations are derived. Wozniak et at. *(18)* showed that two distinct maxima in pollen concentration can be identified in the US, one during spring and one in fall, which can be consistently identified across all regions of the US. In the following, we will focus on the springtime (March-April-May, MAM) maximum, to which mostly deciduous broadleaf trees contribute. As shown in Fig. 2, the emission of different pollen taxa in this period is strongly temporally correlated, making it difficult to disentangle the effect of a single pollen taxon. Therefore, we decided to simplify our analysis by only using the total pollen concentration observed at the respective stations as a proxy for pollen concentration in the atmosphere.

In the following, we compare cloud properties between high and low pollen conditions. Low pollen conditions are defined as situations where pollen concentration, as measured at the surface, is less than 10 m^{-3}, whereas pollen concentration is considered to be high when pollen concentrations of larger than 60 m^{-3} are observed. The upper threshold of 60 m^{-3} is representative of the mean in total pollen concentration during MAM in the USA (see Fig. 2).

To explore the effects of pollen on cloud glaciation, we first employ data from passive satellite remote sensing, and in a second step, also active remote sensing is used. The advantage of the former is the much larger statistical sample due to the wide swath. The advantage of the latter is a less uncertain determination of the cloud thermodynamic phase. As passive remote sensing dataset, we use ice fraction as a function of cloud-top temperature derived from Moderate Resolution Imaging Spectroradiometer (MODIS) Level-2, Collection 6.1 at a horizontal resolution of 1 km *(19)*. An evaluation of the employed MODIS retrieval algorithm for cloud phase shows good agreement with cloud phase derived from the spaceborne CALIPSO lidar *(20)*, providing confidence in the retrieved ice fraction. Around each pollen station, we consider the MODIS retrievals within a circle with radius of 100 km, inside which we assume the pollen concentration to be represented by the one observed at the surface pollen station. Sensitivity studies demonstrated that the results are independent of the exact choice of radius (not shown).

Figure 3 shows the mean difference in ice fraction as diagnosed from the MODIS dataset for cases with high and low pollen concentrations. We find a maximum in the difference between high and low pollen conditions at around -20 °C, which is most strongly expressed in March and April and is slightly reduced in May. For all months, the positive difference in ice fraction is statistically significant for a cloud top temperature range between -17 °C and -23 °C. This increased ice fraction is in good agreement with the freezing temperature of a water-embedded pollen grain between -15 °C and -25 °C, reported in laboratory studies *(10)*. We would like to remark that for temperature greater than -13 °C, the cloud phase retrieval of MODIS gives large weight towards the liquid phase (supplemental material in *20*), so difference between high and low pollen concentrations are close to zero in that temperature regime.

An important aspect to discuss is the change of sign in the ice fraction difference for temperatures lower than -25 °C. While the difference is negative in March, it is positive in April and May. We argue that probably neither signal is attributable to pollen. Rather, during springtime, the atmospheric stratification is becoming increasingly unstable with time and, therefore, more convective, causing an alteration in cloud microphysical properties. This transition can be identified when comparing cloud ice fractions at the end and beginning of each month, where the difference in ice fraction is always negative for the springtime months (fig. S2). As pollen concentration is strongly increasing throughout March and is decreasing throughout April and May (Fig. 2), sampling for high and low pollen condition also implies an implicit temporal sampling. For that reason, the positive cloud ice fraction differences in March for temperatures less than -25 °C can be attributed to a negative temporal trend in cloud ice fraction towards the end of the month. This signal flips in sign in April and May, as there is now a decreasing trend in pollen emission towards the end of the month. Looking at geographical differences in ice fraction (fig. S3), we find that the reported signals in ice fraction for temperatures less then -25 °C mainly stem from eastern USA, where the reduction in ice fraction in March can mainly be attributed to northeastern part of the USA, whereas the southeastern part is causing the enhanced ice fraction.

As also other aerosol species like dust may act as INP in the temperature range where pollen are ice active, we further investigated whether the presence of pollen is spatiotemporally correlated with other aerosols. We compared the pollen concentration observed at the pollen station with the column load of other aerosol species from the Copernicus Atmospheric Monitoring Service (CAMS; *21*), which assimilated MODIS aerosol retrievals *(22)* into the model of the European Centre for Medium-Range Weather Forecasts *(23)*. No or only a weak, but negative correlation of pollen with other aerosol species is found (fig. S4). As pollen and general aerosol load seem to be slightly negatively correlated, the positive signals in the difference in ice fraction in April and May, when pollen concentration is already decreasing but the general aerosol load is increasing (not shown), can potentially be related to other aerosol species that act as INP for temperatures less than -25 °C, which seems to particularly effect the southeastern USA.

To verify the results from MODIS, we additionally employed data from active satellite remote sensing. We use DARDAR (raDAR/liDAR; *24*), which combines information from a spaceborne cloud radar (CloudSat; *25*) and cloud lidar (CALIPSO; *26*). In particular, we utilize the so-called DARDAR_MASK product, which contains information on atmospheric features like the phase state of hydrometeors as well as the presence of atmospheric aerosols. The difference in cloud ice fraction as a function of cloud top temperature for DARDAR is shown in fig. S5. We again find an increased ice fraction which peaks at -20 °C. While the maximum is in accordance with the MODIS-derived difference in ice fraction, the DARDAR-derived positive difference in ice fraction extends towards warmer temperatures

up to the freezing point. The difference to MODIS can be related to the more sensitive cloud phase retrieval of DARDAR with respect to ice clouds especially at temperatures greater than -10 °C. According to laboratory studies, pollen are not considered to be strongly ice active at such elevated temperatures, so this signal can potentially be related to aerosol species like bacteria and/or fungal spores, which are ice active in this temperature regime (e.g., *27,28*) or to aforementioned cross-correlation with meteorological conditions.

Using the ability of DARDAR to penetrate through optically thick clouds and to retrieve information on cloud and hydrometeor properties almost down to the surface, we are able to assess whether an effect of the increased ice fraction due to presence of pollen on precipitation can be identified. As most precipitation over the continents stems from the ice phase (*1*), it is expected that the enhanced cloud ice fraction in response to a higher atmospheric pollen concentration leads to an increase of the fraction of clouds that precipitate. While for low pollen concentrations the fraction of precipitating clouds is 9.19 % ± 0.37 %, it increases to 11.82 % ± 0.19 % for high pollen concentrations, where the given uncertainty is the 95 % confidence interval of the mean derived from bootstrapping with a sample size of 10000. We remark that not all of this increase is causally linked to the increase in ice-containing clouds. Alternative causes are a temporal correlation between the seasonal shift in precipitation frequency and pollen concentration as discussed for cloud ice fraction. Also, the opposite causality exists: precipitation affects pollen concentration in the atmosphere. While precipitation reduces the amount of aerosol in the atmosphere through wet deposition, it has also been demonstrated that pollen concentrations can even increase before and during rainfall events (*29*). A reason for this is that pollen can get lifted by higher winds speed before and during rainfall events. To be able to directly relate alteration in cloud ice fraction between high and low pollen concentrations to alteration in precipitation frequency, we calculated how this change translates into changes in precipitation frequency, given the cloud distribution by temperature and the change in precipitation probability (see materials and methods). We find, as expected, a smaller effect of pollen on the fraction of precipitating clouds from 9.53 % ± 0.02 % for low pollen cases to 10.13 % ± 0.01 % for high pollen cases. This still is a substantial absolute increase by 0.6 % in rain frequency due to the alteration in cloud glaciation over the continental USA during springtime.

Anthropogenic climate change has already been shown to shift the start of springtime pollen emissions, lengthen the pollen season and increase the concentration of airborne pollen (*30,31*). These trends will continue to manifest themselves towards the end of the century due to increased temperatures, changes in precipitation amount and frequency and fertilizing effect of a higher CO_2 concentration (*32*). Our results show that those changes can, at least regionally and during springtime, have a significant effect on cloud glaciation leading to an increase in precipitation frequency. The circumstance that several taxonomic groups of trees jointly produce the distinct peak in pollen production during MAM points to a potential role of biodiversity in controlling cloud glaciation and precipitation which demands further research.

References and Notes

1. J. Mülmenstädt, O. Sourdeval, J. Delanoë, J. Quaas, Frequency of occurrence of rain from liquid-, mixed-, and ice-phase clouds derived from A-Train satellite retrievals. *Geophysical Research Letters* **42**, 6502-6509 (2015).
2. P. R. Field, A. J. Heymsfield, Importance of snow to global precipitation. *Geophysical Research Letters* **42**, 9512-9520 (2015).

3. K. Diehl, C. Quick, S. Matthias-Maser, S. K. Mitra, R. Jaenicke, The ice nucleating ability of pollen Part I: Laboratory studies in deposition and condensation freezing modes. *Atmospheric Research* **58**, 75-87 (2001).
4. K. Diehl, S. Matthias-Maser, R. Jaenicke, S. K. Mitra, The ice nucleating ability of pollen: Part II. Laboratory studies in immersion and contact freezing modes. *Atmospheric Research* **61**, 125-133 (2002).
5. N. von Blohn, S. K. Mitra, K. Diehl, S. Borrmann, The ice nucleating ability of pollen: Part III: New laboratory studies in immersion and contact freezing modes including more pollen types. *Atmospheric Research* **78**, 182-189 (2005).
6. B. G. Pummer, H. Bauer, J. Bernardi, S. Bleicher, H. Grothe, Suspendable macromolecules are responsible for ice nucleation activity of birch and conifer pollen. *Atmospheric Chemistry and Physics* **12**, 2541-2550 (2012).
7. S. Augustin, H. Wex, D. Niedermeier, B. Pummer, H. Grothe, S. Hartmann, L. Tomsche, T. Clauss, J. Voigtländer, K. Ignatius, F. Stratmann, Immersion freezing of birch pollen washing water. *Atmospheric Chemistry and Physics* **13**, 10989-11003 (2013).
8. J. D. Hader, T. P. Wright, M. D. Petters, Contribution of pollen to atmospheric ice nuclei concentrations. *Atmospheric Chemistry and Physics* **14**, 5433-5449 (2014).
9. V. R. Després, J. Alex Huffman, S. M. Burrows, C. Hoose, A. S. Safatov, G. Buryak, J. Fröhlich-Nowoisky, W. Elbert, M. O. Andreae, U. Pöschl, R. Jaenicke, Primary biological aerosol particles in the atmosphere: A review. T*ellus, Series B: Chemical and Physical Meteorology* **64**, 15598 (2012).
10. E. Gute, J. P. Abbatt, Ice nucleating behavior of different tree pollen in the immersion mode. *Atmospheric Environment* **231**, 117488 (2020).
11. S. Bohlmann, X. Shang, V. Vakkari, E. Giannakaki, A. Leskinen, K. E. Lehtinen, S. Pätsi, M. Komppula, Lidar depolarization ratio of atmospheric pollen at multiple wavelengths. *Atmospheric Chemistry and Physics* **21**, 7083-7097 (2021).
12. V. T. Phillips, P. J. DeMott, C. Andronache, An empirical parameterization of heterogeneous ice nucleation for multiple chemical species of aerosol. *Journal of the Atmospheric Sciences* **65**, 2757-2783 (2008).
13. A. L. Steiner, S. D. Brooks, C. Deng, D. C. Thornton, M. W. Pendleton, V. Bryant, Pollen as atmospheric cloud condensation nuclei. *Geophysical Research Letters* **42**, 3596-3602 (2015).
14. M. C. Wozniak, F. Solmon, A. L. Steiner, Pollen Rupture and Its Impact on Precipitation in Clean Continental Conditions. *Geophysical Research Letters* **45**, 7156-7164 (2018).
15. E. F. Mikhailov, M. L. Pöhlker, K. Reinmuth-Selzle, S. S. Vlasenko, O. O. Krüger, J. Fröhlich-Nowoisky, C. Pöhlker, O. A. Ivanova, A. A. Kiselev, L. A. Kremper, U. Pöschl, Water uptake of subpollen aerosol particles: Hygroscopic growth, cloud condensation nuclei activation, and liquid-liquid phase separation. *Atmospheric Chemistry and Physics* **21**, 6999-7022 (2021).
16. J. Burkart, J. Gratzl, T. M. Seifried, P. Bieber, H. Grothe, Isolation of subpollen particles (SPPs) of birch: SPPs are potential carriers of ice nucleating macromolecules. *Biogeosciences* **18**, 5751-5765 (2021).

17. T. M. Seifried, P. Bieber, A. T. Kunert, D. G. Schmale, K. Whitmore, J. Fröhlich-Nowoisky, H. Grothe, Ice nucleation activity of alpine bioaerosol emitted in vicinity of a birch forest. *Atmosphere* **12**, 799 (2021).

18. M. C. Wozniak, A. L. Steiner, A prognostic pollen emissions model for climate models (PECM1.0). *Geoscientific Model Development* **10**, 4105-4127 (2017).

19. S. Platnick, K. G. Meyer, M. D. King, G. Wind, N. Amarasinghe, B. Marchant, G. T. Arnold, Z. Zhang, P. A. Hubanks, R. E. Holz, P. Yang, W. L. Ridgway, J. Riedi, The MODIS Cloud Optical and Microphysical Products: Collection 6 Updates and Examples from Terra and Aqua. *IEEE Transactions on Geoscience and Remote Sensing* **55**, 502-525 (2017).

20. B. Marchant, S. Platnick, K. Meyer, G. Thomas Arnold, J. Riedi, MODIS Collection 6 shortwave-derived cloud phase classification algorithm and comparisons with CALIOP. *Atmospheric Measurement Techniques* **9**, 1587-1599 (2016).

21. A. Inness, M. Ades, A. Agustí-Panareda, J. Barré, A. Benedictow, A.-M. Blechschmidt, J.J. Dominguez, R. Engelen H. Eskes, J. Flemming, V. Huijnen, L. Jones, Z. Kipling, S. Massart, M. Parrington, V.-H. Peuch, M. Razinger, S. Remy, M. Schulz, M. Suttie, The CAMS reanalysis of atmospheric composition. *Atmospheric Chemistry and Physics* **19**, 3515-3556 (2019).

22. R. C. Levy, S. Mattoo, L. A. Munchak, L. A. Remer, A. M. Sayer, F. Patadia, N. C. Hsu, The Collection 6 MODIS aerosol products over land and ocean. *Atmospheric Measurement Techniques* **6**, 2989-3034 (2013).

23. A. Benedetti, J.-J. Morcrette, O. Boucher, A. Dethof, R. J. Engelen, M. Fisher, H. Flentje, N. Huneeus, L. Jones, J. W. Kaiser, S. Kinne, A. Mangold, M. Razinger, A. J. Simmons, M. Suttie, Aerosol analysis and forecast in the European Centre for Medium-Range Weather Forecasts Integrated Forecast System: 2. Data assimilation. *Journal of Geophysical Research* **114**, D13205 (2009).

24. J. Delanoë, R. J. Hogan, Combined CloudSat-CALIPSO-MODIS retrievals of the properties of ice clouds. *Journal of Geophysical Research Atmospheres* **115**, 1-17 (2010).

25. G. L. Stephens, D. G. Vane, R. J. Boain, G. G. Mace, K. Sassen, Z. Wang, A. J. Illingworth, , E. J. O'Connor, W. B. Rossow, S. L. Durden, S. D. Miller, R. T. Austin, A. Benedetti, C. Mitrescu, The CloudSat mission and the A-Train: A new dimension of space-based observations of clouds and precipitation. *Bulletin of the American Meteorological Society* **83**, 1771-1790 (2002).

26. D. M. Winker, J. R. Pelon, M. P. McCormick, The CALIPSO mission: Spaceborne lidar for observation of aerosols and clouds. *Proc. of SPIE* **4893**, 1-11 (2003).

27. B. J. Murray, D. O'Sullivan, J. D. Atkinson, M. E. Webb, Ice nucleation by particles immersed in supercooled cloud droplets. *Chemical Society Reviews* **41**, 6519-6544 (2012).

28. Z. A. Kanji, L. A. Ladino, H. Wex, Y. Boose, M. Burkert-Kohn, D. J. Cziczo, M. Krämer, Overview of Ice Nucleating Particles. *Meteorological Monographs* **58**, 1.1-1.33 (2017).

29. K. Kluska, K. Piotrowicz, I. Kasprzyk, The impact of rainfall on the diurnal patterns of atmospheric pollen concentrations. *Agricultural and Forest Meteorology* **291**, 108042 (2020).

30. L. H. Ziska, L. Makra, S. K. Harry, N. Bruffaerts, M. Hendrickx, F. Coates, A. Saarto, M. Thibaudon, G. Oliver, A. Damialis, A. Charalampopoulos, D. Vokou, S. Heiđmarsson, E. Guđjohnsen, M. Bonini, J.-W. Oh, K. Sullivan, L. Ford, G. D. Brooks, D. Myszkowska, E. Severova, R. Gehrig, G. D. Ramón, P. J. Beggs, K. Knowlton, A. R. Crimmins, Temperature-related changes in airborne allergenic pollen abundance and seasonality across the northern hemisphere: a retrospective data analysis. *The Lancet Planetary Health* **3**, e124-e131 (2019).

31. W. R. L. Anderegg, J. T. Abatzoglou, L. D. L. Anderegg, L. Bielory, P. L. Kinney, L. Ziska, Anthropogenic climate change is worsening North American pollen seasons. *Proceedings of the National Academy of Sciences* **118**, 1-6 (2021).

32. Y. Zhang, A. L. Steiner, Projected climate-driven changes in pollen emission season length and magnitude over the continental United States. *Nature Communications* **13**, 1-10 (2022).

33. J. Nowosad, A. Stach, I. Kasprzyk, Ł. Grewling, M. Latałowa, M. Puc, D. Myszkowska, E. Weryszko-Chmielewska, K. Piotrowska-Weryszko, K. Chłopek, B. Majkowska-Wojciechowska, A. Uruska, Temporal and spatiotemporal autocorrelation of daily concentrations of Alnus, Betula, and Corylus pollen in Poland. *Aerobiologia* **31**, 159-177 (2015).

34. M. Sofiev, On impact of transport conditions on variability of the seasonal pollen index, *Aerobiologia* **33**, 167–179 (2017)

Acknowledgments: We thank all the AAAAI National Allergy Bureau pollen station data providers. The authors thank Tom Goren for valuable discussion regarding the MODIS data.

Funding: All author's received direct funding from their respective institution, which is gratefully acknowledged.

Author contributions:

Conceptualization: JK, JQ

Methodology: JK, CW, MP, FS, HW, JQ

Investigation: JK, JQ

Visualization: JK, MP, JQ

Supervision: JQ

Writing – original draft: JK

Writing – review & editing: JK, CW, MP, FS, HW, JQ

Competing interests: The authors declare that they have no competing interests.

Data and materials availability:

The MODIS Aqua/Terra cloud products are publicly available from the Atmosphere Archive and Distribution System (LAADS) Distributed Active Archive Center (http://dx.doi.org/10.5067/MODIS/MOD06_L2.061 and http://dx.doi.org/10.5067/MODIS/MYD06_L2.061). The DARDAR data used are available from the AERIS ICARE data center (https://www.icare.univ-lille.fr/dardar/overview-dardar-mask/; last accessed 13.02.2023). Access to the pollen

station data is license protected can be requested from the National Allergy Bureau (https://allergist.aaaai.org/forms/nab-data-request-form.php; last accessed 13.02.2023)

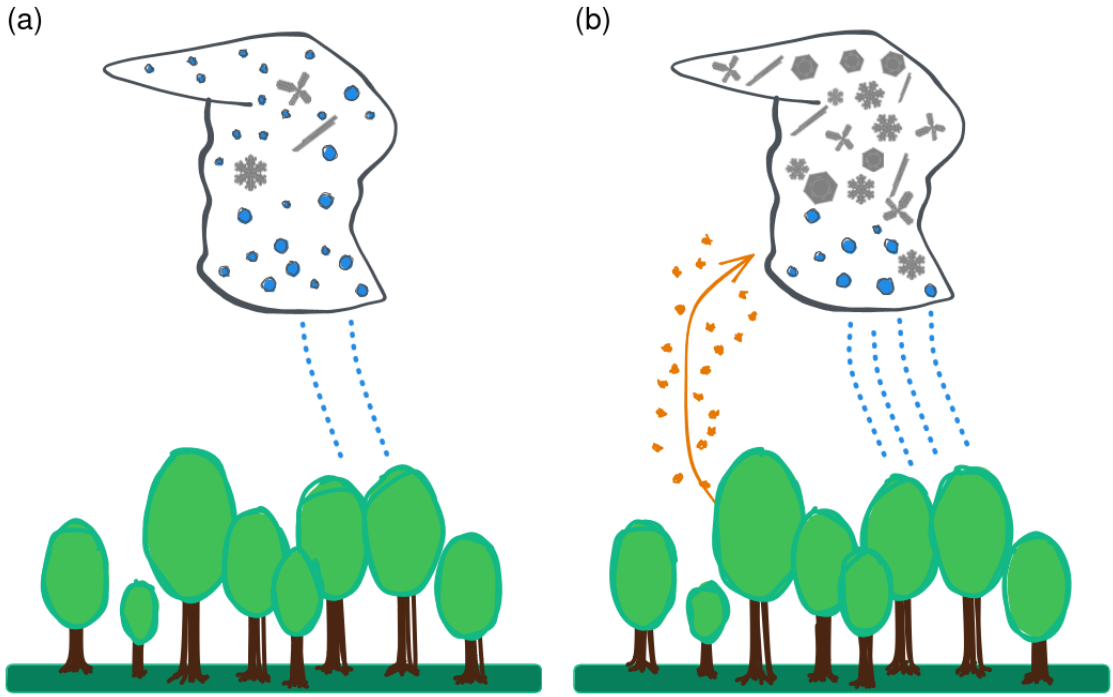

Fig. 1. Schematic depiction of the proposed glaciating effect of pollen on mixed-phase clouds. During pollen season (b), cloud ice fraction is increased compared to situations with low pollen concentration (a), consequently leading to an increase in rain frequency.

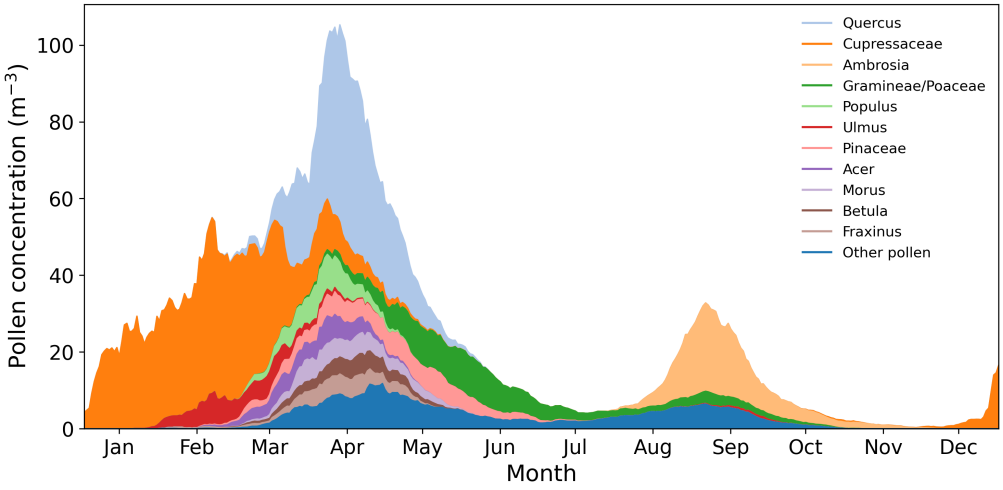

Fig. 2. Median of pollen concentration for multi-year averaged seasonal cycle at all pollen stations used in this study. A seven-day running mean was applied for smoothing the time series. The eleven most frequently counted pollen taxa are shown at a genus or family resolution. All other pollen taxa are subsumed under "Other pollen".

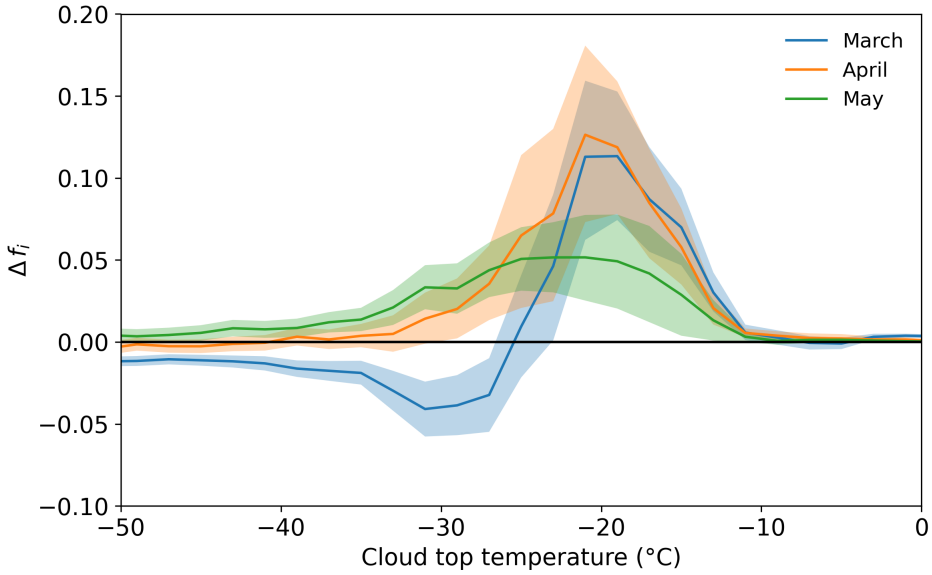

Fig. 3. MODIS-derived mean difference in ice fraction Δf_i between high and low pollen concentrations as a function of cloud-top temperature. Δf_i is binned every 2 K and data are averaged for ten years from 2007 to 2016. MODIS data are sampled within a radius of 100 km around each pollen station. Low pollen cases are defined as having a total pollen concentration at the station of less than 10 m^{-3} and high pollen cases are defined as having a total pollen concentration at the station of greater than 60 m^{-3}. Shaded areas indicate the 95 % confidence interval of the mean as estimated from bootstrapping using a sample size of 10000.

Supplementary Materials

Materials and Methods

We employ ground-based pollen concentration data collected from stations within the United States (US) (the location of pollen stations used is given in Fig. S1). Pollen station data are disseminated by the National Allergy Bureau (NAB), which is part of the American Academy of Allergy, Asthma and Immunology (AAAAI). In this study, we use pollen concentrations collected by more than 50 surface stations in a period from 2007 to 2017. Each timeseries at a station contains pollen concentrations of up to 40 different pollen taxa, but due to a strong temporal correlation in pollen emission, we simplify the analysis by only using total pollen concentration in our analysis. We need to remark that not all stations cover the full time period of interest, but cloud properties in the vicinity of a pollen station are only sampled if information on pollen concentration is available. We chose a radius of 100 km around a pollen station where we sample cloud properties from satellite products as we consider pollen emission in a region to be spatiotemporally homogeneous. Such conditions can to some extent be assumed for regional scales of a few hundred kilometers with similar climatic conditions and similar composition of pollen emitting plants *(33)*. We nevertheless do not want to overextend this assumption, as long-range transport clearly has been shown to decorrelate observed pollen concentrations from local emissions *(34)*. For that reason, we evaluated the effect of using different sampling radii around the pollen stations for cloud properties from the satellites, but the findings in this study were independent of the employed sampling radius.

We use daily data from the Moderate Resolution Imaging Spectroradiometer (MODIS) Level-2, Collection 6.1 dataset at a horizontal resolution of 1 km, from both, the Aqua and Terra satellites. Due to the wide swath of MODIS, a large number of satellite pixels are available in the vicinity of a pollen station, which enables us to calculate cloud ice fraction f_i as a function of temperature *(T)* at each station and timestep. At each cloudy satellite pixel, the MODIS cloud phase retrieval indicates if a cloud is liquid or ice or if the cloud phase retrieval is uncertain. Due to the fact that the cloud phase retrieval in the MODIS dataset is dependent on information from shortwave spectral bands, we only use daytime overpasses in our analysis. Furthermore, we only consider pixels that are flagged as single-layer clouds by the MODIS retrieval to avoid uncertain retrievals in cloud top temperature and phase. From the ratio of pixels in the ice phase to the total number of cloudy pixels within the 100 km sampling radius, we calculate f_i, binned by cloud top temperature at each station *(s)* and each satellite overpass/timesteps *(t)*, defined as:

$$f_i(T,s,t) = \frac{n_{ice}(T,s,t)}{\Sigma_j n_j(T,s,t)}$$

Here we use a bin width of 2 K between –50 °C and 10 °C. To compare high and low pollen cases, we calculate the mean of f_i at each temperature bin among all stations and timesteps, respectively. Here, a weighted mean is employed to give more weight to situations having more cloudy pixels within the sampling radius, such that:

$$\overline{f_i}(T) = \Sigma_{s,t} w(T,s,t) f_i(T,s,t) \text{ with } w(T,s,t) = \frac{\Sigma_j n_j(T,s,t)}{\Sigma_{j,s,t} n_j(T,s,t)}$$

To quantify statistical uncertainty in the difference of $\overline{f_i}(T)$ between high and low pollen cases, we bootstrapped the mean of high and low pollen cases using a sample size of 10000 to calculate the 95 % confidence interval for this difference.
We additionally use information on cloud properties from DARDAR (raDAR/liDAR; *24*), combining data from a spaceborne cloud radar (CloudSat; *25*) and cloud lidar (CALIPSO; *26*). In particular, we use information from the so-called DARDAR_MASK, which contains information on atmospheric features like the phase state of clouds, precipitation and atmospheric aerosols. The fact that information on atmospheric features are sampled along the ground track of the two satellites drastically limits the number of available data points in the vicinity of a pollen station. For that reason, we only look at the entire springtime period (MAM), increased the sampling radius to 200 km, and additionally increased the width of the temperature bins to 10 K. As DARDAR employs information from active sensors that are independent of insolation, we additionally use nighttime overpasses to increase the number of available overpasses over pollen stations. To be comparable to MODIS, we first have to detect cloud top in the DARDAR dataset. To avoid spurious detection of a cloud layer in DARDAR, at least four consecutive cloudy points within each vertical profile (which is equivalent to a geometrical cloud depth of at least 240 m) have to be present. The cloud phase at cloud top is then considered in the ice fraction calculation. We only use situations where only one single cloud top is detected in DARDAR to be comparable to MODIS data, where we also only consider single-layer clouds. While MODIS actually infers cloud top temperature from observed radiances, cloud top temperature in DARDAR is derived from ECMWF-AUX, the spatially interpolated meteorological analysis of the European Centre for Medium-Range Weather Prediction (ECMWF). MODIS only distinguishes between liquid and ice clouds, whereas in DARDAR also mixed-phase clouds (ice+supercooled) can be detected, which we consider to be in the liquid phase. Due to the limited amount of data points along the satellite ground track in the vicinity of pollen stations, we do not calculate ice fraction for a single pollen station, but calculate $\overline{f_i}$ along the whole ground track:

$$\overline{f_i}(T) = \frac{n_{ice}(T)}{\Sigma_j n_j(T)} \quad j \in \{\text{ice,mixed-phase,supercooled,liquid}\},$$

where n_j is the number of pixels of the respective cloud phase category.
Using the ability of DARDAR to penetrate through optically thick clouds and to retrieve information on cloud and hydrometeor properties almost down to the surface, we are furthermore able to assess whether an effect of pollen on precipitation can be identified. We quantify this by comparing the fraction of precipitation clouds for high and low pollen situations. As information on whether a cloud is precipitating is derived from CloudSat, which suffers from ground clutter, we assume a cloud to be precipitating when the DARDAR_MASK profile indicates precipitation at 500 m above ground level. Using this information, we calculate the ratio of precipitating clouds $\overline{f_p}$ for temperatures between –50 °C and 10 °C. Besides the directly derived fraction of precipitating clouds, we recalculate this value from changes in ice fraction, enabling us to quantify the effect of modified ice fraction on precipitation when pollen are present. Any deviation for the directly calculated precipitation fraction is indicative of other processes that influence rain fraction besides the glaciating effect of pollen. The total fraction of precipitating clouds can then be calculated as follows:

$$\overline{f_p}(T) = \overline{f_i}(T)p_{ice}(T) + [1 - f_i(T)]p_{liq},$$

where $p_{ice}(T)$ / $p_{liq}(T)$ is the fraction of ice/liquid clouds that precipitate at a temperature bin, which we calculated from all available DARDAR profiles in the USA from 2007 to 2016. We again employ a weighted mean to calculate the mean fraction of precipitating clouds for all temperature bins from –50 °C and 10 °C:

$$\overline{f_{p,calc}} = \Sigma_T w(T) f_p(T)$$

where $w(T)$ is the ratio of cloudy profiles to the number of cloudy profiles in that temperature bin.

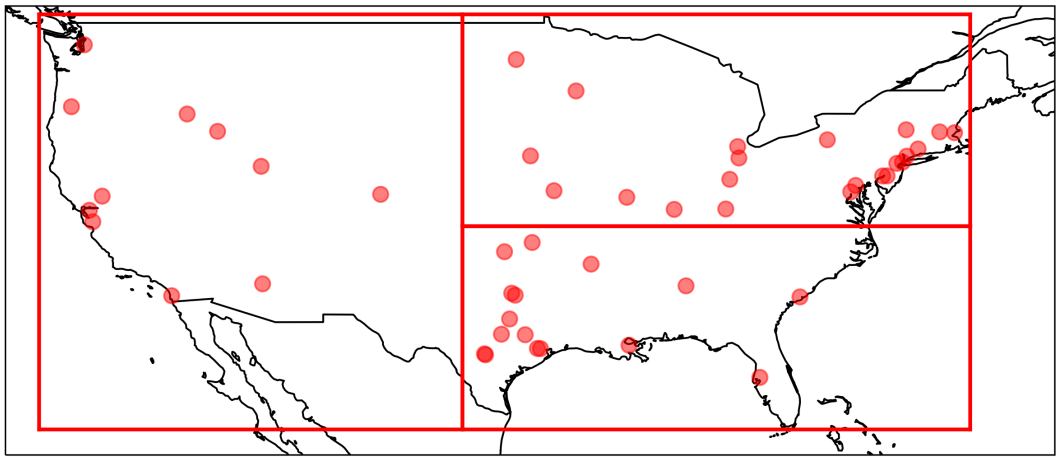

Fig. S1.
Location of ground-based pollen stations used in the analysis.

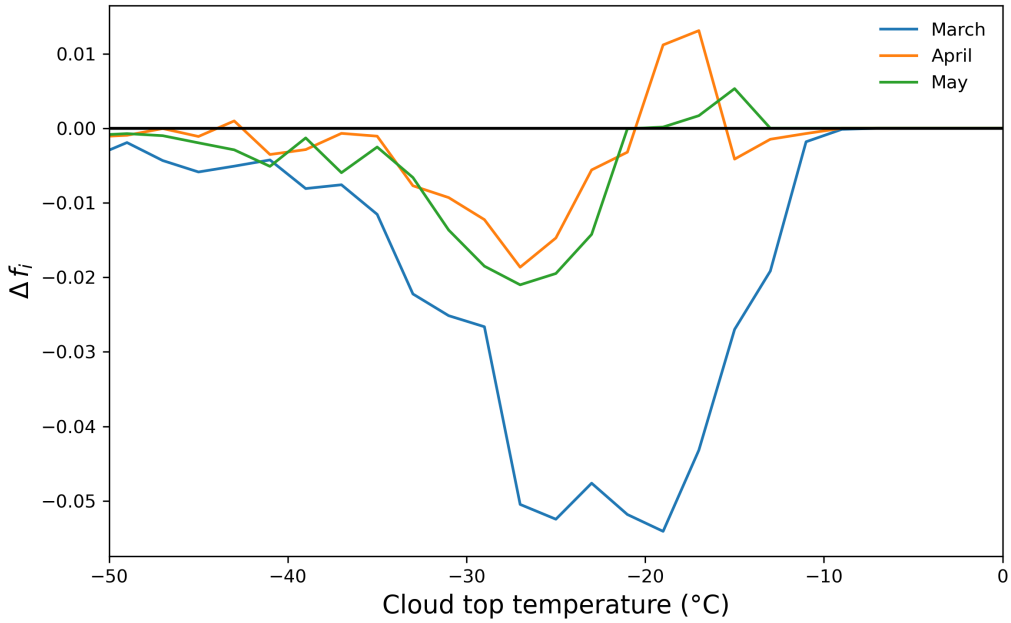

Fig. S2.

Multi-year monthly averaged MODIS ice fraction difference Δf_i between the last and the first ten days of the respective month, averaged over all pollen stations.

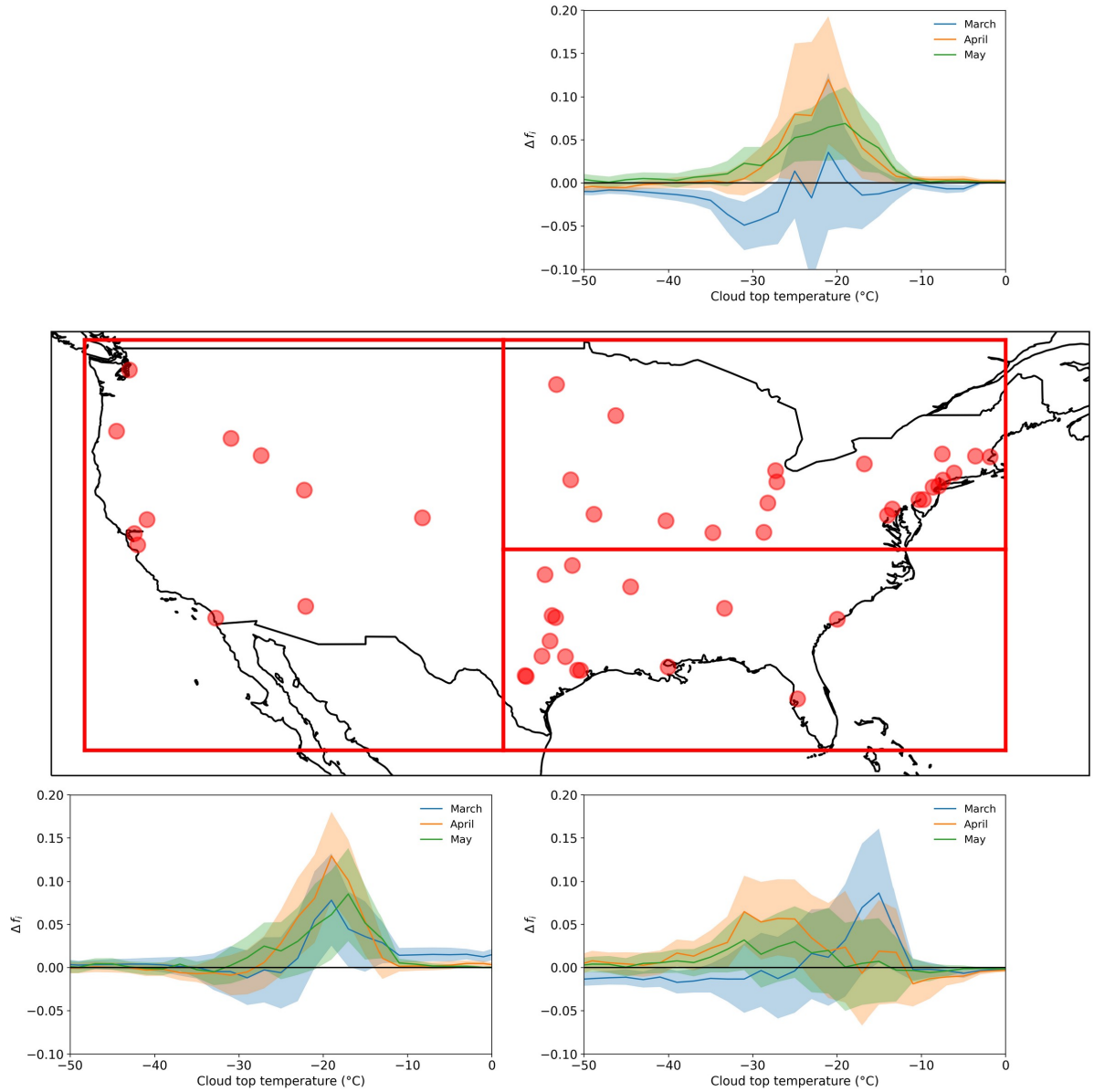

Fig. S3.
As Fig. 3 but for the three geographical regions, indicated by the red boxes.

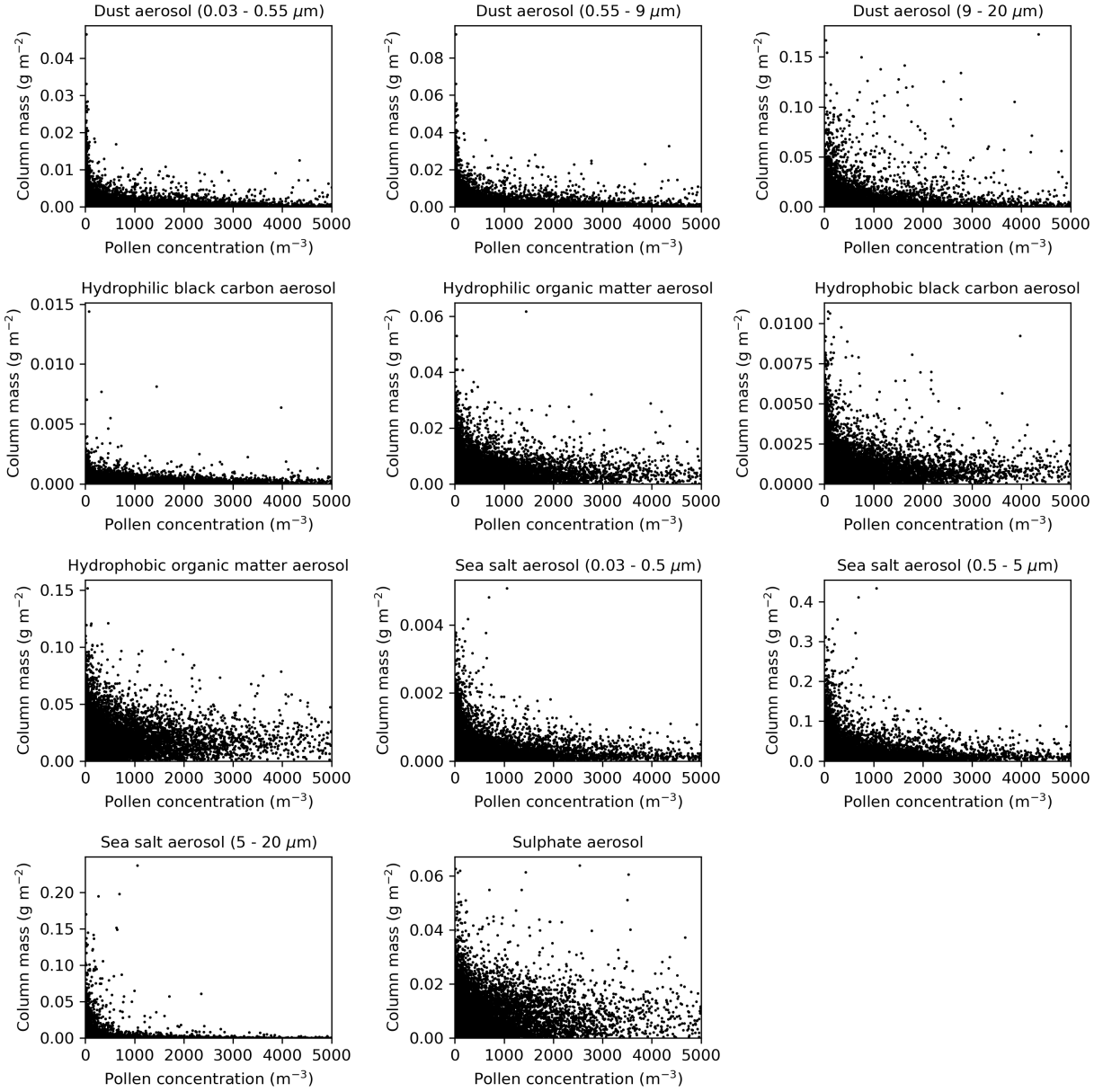

Fig. S4.
Scatter plots correlating column mass of different aerosol species from the CAMS aerosol reanalysis to ground based pollen concentration for springtime (March-April-May). CAMS reanalysis data is spatiotemporally sampled to data at the pollen stations.

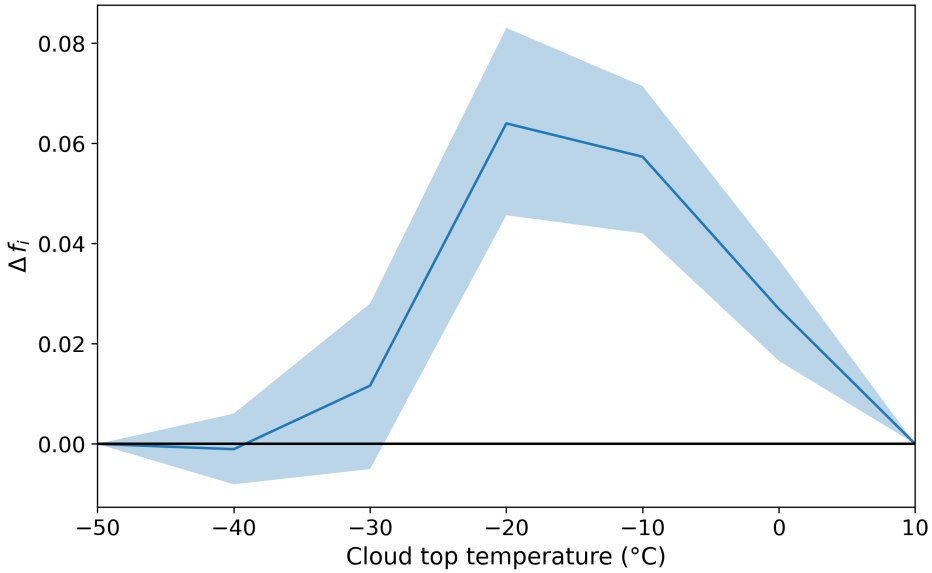

Fig. S5.
As Fig. 3, but from DARDAR active satellite remote sensing retrievals, sampled within a radius of 200 km around each pollen station, using 10 K bins in cloud temperature, and considering the MAM period.